# Design of a Planar Cavity Resonator for 12.5 GHz Low Phase Noise SiGe HBT Oscillator

Jae-Won Lee[1] · Yong-Hoon Kim[2]

## Abstract

In this paper, the novel microwave oscillator incorporating a planar cavity resonator(PCR) is presented to reduce the phase noise of the oscillator in a planar environment. Compared to the conventional planar( $\lambda/4$ open stub resonator), the phase noise is improved about 16 dBc/Hz @100 kHz. The design of the oscillator is based on a reflection type configuration using the low 1/f SiGe HBT transistor(LPT16ED). The output power is measured 2.76 dBm at 12.5 GHz. In this paper, the oscillator used to the PCR can be expected to provide a solution for low phase noise oscillator in microwave circuits.

***Key words*** : Planar Cavity Resonator, Microstrip Resonator, HBT, MEMS, MMIC.

## I . Introduction

The number of radio frequency applications has steadily increased with demanding for more bandwidth and higher data-rates which are shifting the carrier frequencies to higher values. A Ku-band has been used in a satellite communication since the end of 1970'. In the satellite communication, the low phase noise frequency synthesizer is essential element to implement high quality communication link.

Both the low 1/f noise of a device and the high quality factor of a resonator are very important factors to reduce the phase noise. SiGe HBT has good characteristics of low-frequency 1/f noise compared to other devices such as MESFET and HEMT[1]~[3]. Therefore, the SiGe HBT(LPT16ED) produced by SiGe semiconductor, Inc. is chosen. Many kinds of the resonators have studied to reduce the phase noise. Dielectric resonators have been widely used for low phase noise, but it can not be used to monolithic microwave integrated circuit. The microstrip resonators have the advantages such as high integration, low cost and simply manufacturing. However it can not mainly affect to reduce the phase noise of oscillator, due to the low $Q$ of the resonator. Therefore, the micromachined cavities of the planar type have be developed[4]~[6]. This resonator is asked to have a high skill manufacturing process and the high cost of the beginning development stage.

In Fig. 1, planar cavity resonator(PCR) oscillator consists in two kinds of the substrates(duroid 5880, $\varepsilon_r$ =2.2) which are different from thickness. The circuit is

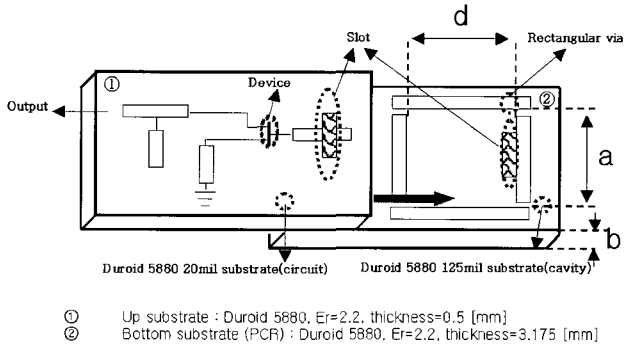


Fig. 1. The topology of the suggested PCR oscillator.

fabricated on the up substrate and the PCR on the bottom substrate. As the rectangular via is in the role of the cavity's metallic wall, the size of the PCR is decided by length $d$, width $a$ and height $b$. Coupling between cavity and the microstrip line is achieved with the slot on the ground plane of the microstrip line.

The main contributions of this PCR are following. First, we can obtain the higher $Q$ of the resonator than that of other microstrip resonators. Second, it has the advantage of a planar form which is easy to integrate with microwave integrate circuit(MIC). Because the cavity substrate is placed at the bottom of circuit substrate, it is easy to make integration better. Third, there is easy-fabrication process, because of the conventional PCB processing.

## II . Selection of the Optimum Cavity Size

Manuscript received May 16, 2005 ; revised September 23, 2005. (ID No. 20050516-019J)

[1]Samsung Thales Co., Ltd, Yongin, Korea.
[2]Department of Mechatronics, Gwangju Institute of Science Technology, Gwangju, Korea.

When the wanted cavity resonator is designed, the quality factor($Q$) and the mode characteristic of the resonator must be taken into account. Through the following design process, the excitation of spurious modes is minimized and the $Q$ is maximized. The higher the $Q$ of the resonator is, the more stable the oscillator can be. The adjacent mode of the dominant mode should be as far as possible to increase the selectivity of oscillator frequency. It is relative to the dimension of resonator. In Fig. 1, it consists of the length d, the width a and the height b of cavity's size.

$$f_{nml}=\frac{ck_{mnl}}{2\pi\sqrt{\mu_r\varepsilon_r}}=\frac{c}{2\pi\sqrt{\mu_r\varepsilon_r}}\sqrt{\left(\frac{m\pi}{a}\right)^2+\left(\frac{n\pi}{b}\right)^2+\left(\frac{l\pi}{d}\right)^2} \quad (1)$$

$$Q_o=\frac{2\omega_0 W_e}{P_c}=\frac{(kad)^3 b\eta}{2\pi^2 R_s(2l^2a^3b+2bd^3+l^2a^3d+ad^3)} \quad (2)$$

At equation (1), when the $TE_{101}$ of the dominant mode is 12.5 GHz, we can have the union of a and d in $11.5\leq d\leq 25$ mm, $b$=3.175 mm in Table 1. According to this union, we can again get the harmonics at the dominant frequency 12.5 GHz from equation (1).

Fig. 2 shows the mode chart for a rectangular cavity with the variation of length $a$ and $d$, when $TE_{101}$ mode resonant frequency is 12.5 GHz at $b$=3.175 mm. The farthest distance between the dominant mode($TE_{101}$) and the second harmonic($TE_{102}$) must be selected to minimize the excitation of spurious modes. Simultaneously, the $Q$ of the resonator should be taken into account. The unloaded $Q_O$ can be calculated on equation (2). Fig. 3 shows the relation of the unloaded $Q_O$ and the second harmonic ($TE_{102}$).

As you can see in Fig. 3, the farther the distance between the dominant and the second harmonic is, the higher the unloaded $Q_O$ of the resonator is. Therefore, the relation of the unloaded $Q_O$ and the spurious is

Table 1. According to the size, the second harmonic at $f$=12.5 GHz. ($b$=3.175 mm)

| $d$ [mm] | $a$ [mm] | Dominant Frequency[GHz] | Second Frequency [GHz] |
|---|---|---|---|
| 11.5 | 11.38459 | 12.5 | 19.7 |
| 11.8 | 11.11446 | 12.5 | 19.4 |
| 12 | 10.95499 | 12.5 | 19.2 |
| 12.3 | 10.74143 | 12.5 | 18.9 |
| ... | ... | ... | ... |
| 22.1 | 8.69417 | 12.5 | 14.8 |
| 22.5 | 8.67056 | 12.5 | 14.7 |
| 22.9 | 8.64835 | 12.5 | 14.7 |

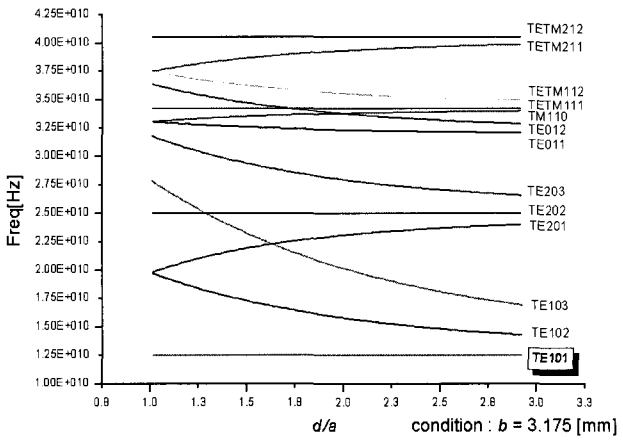


Fig. 2. Mode chart for a rectangular cavity.

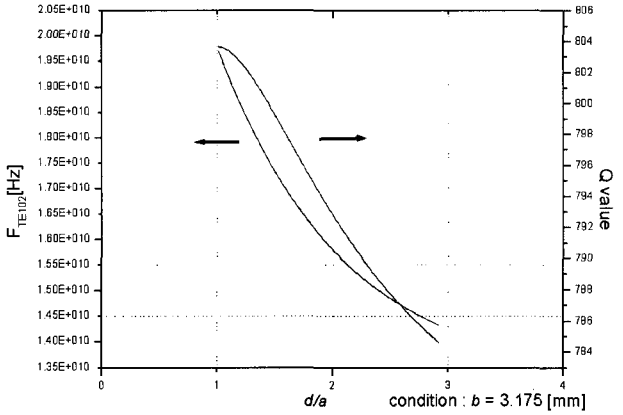


Fig. 3. The relation of the $Q$ and second harmonic at $b$ =3.175 [mm].

proportioned. When the $d$=11.5 [mm] and $a$=11.38 [mm] are selected, the second harmonic is at 19.7 GHz. At this point, the excitation of spurious modes is minimized and the unloaded $Q_O$ is maximized. Therefore, the initial size of the cavity can be decided. These results are verified with the eigemode solver of the FEM simulator(HFSS).

## III. Slot Position

The resonator of the band stop mode must be designed for this topology of the series feedback oscillator. So the coupling between the cavity and the microstrip is occurred at H-field in this resonator. Using full wave field simulation used to the FEM simulator (ansoft HFSS), we can verify the H-field distribution of the cavity. The high H-field distribution is at the near rectangular via in Fig. 4. Therefore, this slot position is selected at the high H-field distribution to get the high coupling.

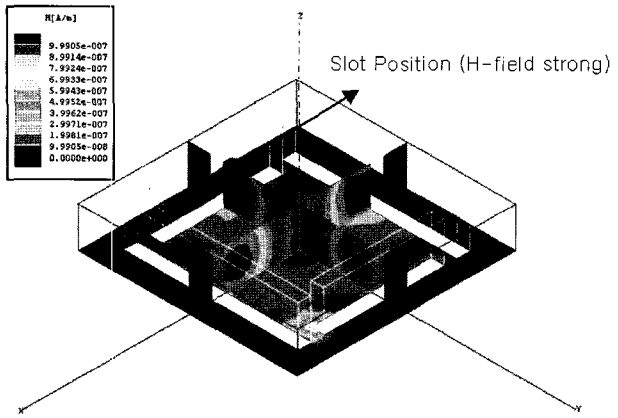


Fig. 4. The H-field distribution of the cavity.

## Ⅳ. Resonator Parameter according to the Slot Size

The important parameters of the resonator such as unloaded $Q_O$, loaded $Q_L$ and coupling coefficient $K$ are analyzed according to the slot size. The magnitude of the $S_{11}$(input reflection at resonator) is important to gratify the oscillation condition. In the conventional DR resonator, these parameters are decided by the distance between the dielectric resonator and the microstrip[7]. But the parameter of this PCR is decided to the size of the slot, due to the fixed circuit thickness. As the slot length is varied from 2.0 to 4.0 mm with varying the slot width from 0.1 to 2.5 mm, these parameters are extracted by using the FEM simulator.

### 4-1 Unloaded $Q_O$ and Loaded $Q_L$

The average value of the unloaded $Q_O$ is 750. According to the large size of the slot, the unloaded $Q_O$ is varied largely. In Fig. 5, we can see that the maximum point is 802 and the minimum point is 550.

In Fig. 6, the values of the loaded $Q_L$ are in inverse proportion to the size of the slot. It is clear that the relation of the k and $Q_L$ is as like in equation (3). The maximum point is 600 and the minimum point is 10.

### 4-2 Coupling Coefficient

The coupling coefficient is the measurement of the degree of coupling between the cavity and the transmission line. When $K$=1, this is a critical coupling. For $K$<1, the cavity is undercoupled to the external component. The cavity and the external component are overcoupled when $K$>1. In Fig. 7, the larger the slot size is, the bigger the coupling coefficient is. The loaded $Q_L$ and the unloaded $Q_O$ are related by the coupling coefficient. The relationship is

$$Q_L = \frac{Q_O}{1+k} \tag{3}$$

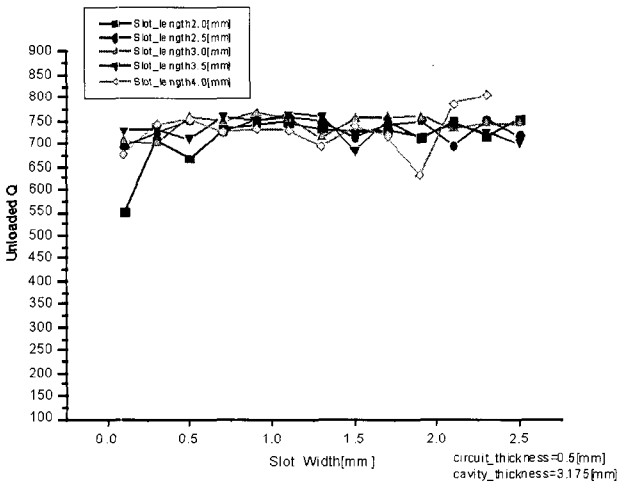


Fig. 5. Unloaded $Q_O$ according to the slot size.

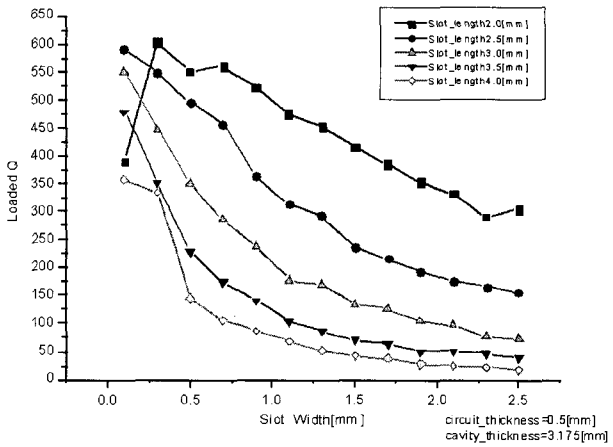


Fig. 6. Loaded $Q_L$ according to the slot size.

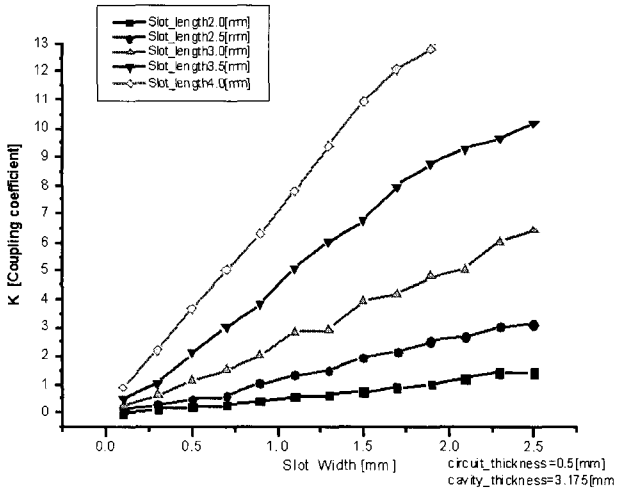


Fig. 7. Coupling coefficient according to the slot size.

If the high $k$ is selected, the loaded $Q_L$ is low, and then the phase noise is degraded. If the lowest $K$ to get the highest loaded $Q_L$ is selected, the oscillator condition in equation (4) can not be satisfied. We need to trade off between the loaded $Q_L$ and the coupling coefficient $K$ at the highest unloaded $Q_O$.

### 4-3 Magnitude of $S_{11}$

When the oscillator is designed, we must think about the magnitude of the $S_{11}$(input reflection at resonator) to satisfy with the initial condition of the oscillator.

$$|S_{11}| > \frac{1}{|S'_{11}|}, \quad phase(S_{11}) = -phase\left(\frac{1}{S'_{11}}\right) \tag{4}$$

Because the $S_{11}'$ of this device is $1.45 \angle -168.492$, $S_{11}$ can be calculated in equation (4). The magnitude of $S_{11}$ must be selected at the upper side of 0.68 in Fig. 8. So the size of a slot is decided to select the 2.5 mm of slot length and the 1.6 mm of slot width.

## V. Designed PCR and Measurement Data

Using the general PCB processing, the planar cavity resonator is manufactured in Fig. 9. Cavity substrate is duriod 5880 which has $\varepsilon_r$=2.2 and thickness=3.175 mm.

In Fig. 10, there is the difference between the simulation and measurement data. It seems to generate the manufacture error and the mismatch of the slots between microstrip and cavity, so it was again simulated according to the change of cavity size for getting the amount

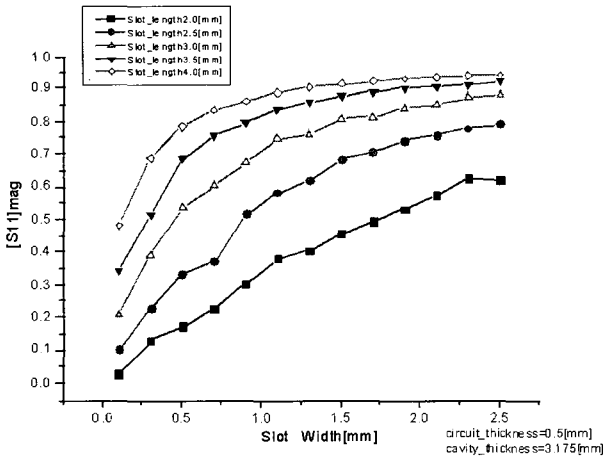


Fig. 8. The magnitude of $S_{11}$ according to the slot size.

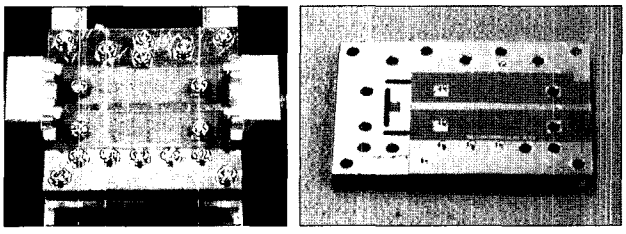

Fig. 9. Photo of designed planar cavity resonator.

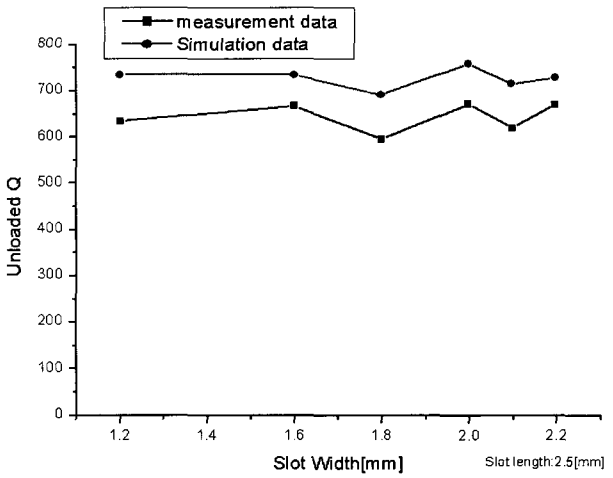


(a) Unloaded

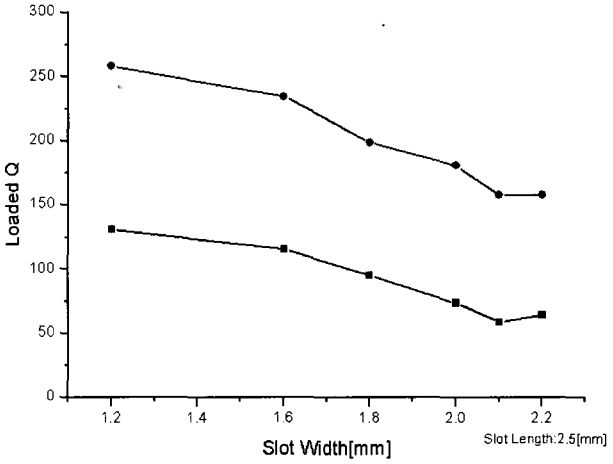


(b) Loaded $Q_L$

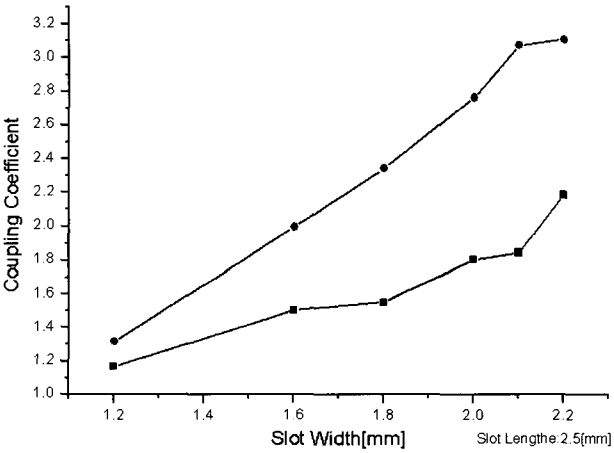


(c) Coupling coefficient

Fig. 10. Measured the parameter of the PCR.

of the resonance frequency shift. As the width of cavity reduces 0.02 mm, the frequency is shifted about +10 MHz. In Fig. 10(b), (c), the average of the unloaded $Q_O$ is 650. The measurement loaded $Q$ is 100 worse than the simulation data.

As mentioned in the previous chapter, the slot width 1.6 mm and length 2.5 mm are selected. In Fig. 11 and Table 2, the simulation data is compared with the measurement data. The $Q$ values of the unloaded and loaded PCR is measured 667.9 and 115.6. The frequency is shifted by the manufacturing error. $Q_L$ is high error as compared with the $Q_O$, due to the slot position error. When the performance of the planar cavity resonator is compared with the existing resonator in Table 3, the loaded $Q$ of the DR is the highest value among them. But the DR is the nonplanar structure. The MSR has the advantage of planar structure. But the MSR has the low unloaded $Q$, due to the radiation and dielectric loss. MEMS resonators using micromaching techniques to eliminate the dielectric loss have the unloaded $Q$ of 500. But it needs to the high processing skill. As a result, the unloaded $Q$ of the planar cavity resonator is much better than that of MSR and MEMS resonator. Although the $Q$ of PCR is lower than that of the DR, there are merits of the easy fabrication, low cost, and the integration capability.

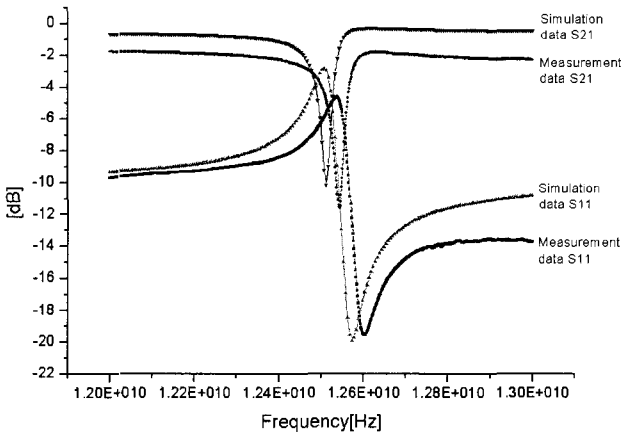


Fig. 11. Simulation and measurement data of designed PCR.

Table 2. The PCR parameter of the simulation and measurement.

| | Simulation | Measurement |
|---|---|---|
| Frequency | 12.51 GHz | 12.51 GHz |
| $K$ | 2.3387 | 1.5 |
| Unloaded $Q$ | 691.4365 | 667.9 |
| Loaded $Q$ | 198.8086 | 115.6 |

Table 3. The comparison of different resonators.

| Type | | Frequency[GHz] | Unloaded Qu |
|---|---|---|---|
| MSR | Hair-pin resonator[10] | 9 | 170 |
| | Spiral resonator[11] | 10 | 146 |
| MEMS | Micromachined cavity resonator[6] | 10.285 | 506 |
| | Membrane resonator[5] | 28.7 | 460 |
| DR | DR resonator[12] | 9.6 | 5000 |
| PCR | This work | 12.56 | 667.9 |

## Ⅵ. Designed Oscillator Using PCR

The topology of oscillator is used for the common emitter series feedback. The series feedback is better than the parallel feedback about low phase noise[8]. Another oscillator is designed by using a conventional MSR( $\lambda/4$ open stub resonator) to investigate the performance. The same circuit substrate(duroid 5880, $Er$ =2.2, thickness=0.5 mm) and the same device(LPT16-ED) are used.

Fig. 12 shows the designed PCR oscillator. Two substrates are aligned by several halls and are fixed by several screws. The performance of PCR oscillator is measured by the test fixture. When a RF cable loss is considered, the output power of the oscillator was 2.76 dBm at $Ib$(Tr base current)=497 $\mu$A and $Vce$(Tr currect and emmiter voltage)=3 V in Fig. 13. The corresponding dc-RF efficiency is around 2 %. In Fig. 14, the phase noise measured is 109.23 dBc/Hz at the 100 kHz offset.

When the base current is swept from 0.3 to 0.7 mA at $Vce$=3 V, the base current dependence of the output power, frequency deviation and phase noise is shown in Fig. 16, Fig. 17. This PCR oscillator is stable within the range of the base current which varies from 0.3 mA to 0.55 mA. In Table 4, measurement shows reduced phase noise by 17.61 dB dBc/Hz @1 MHz offset in the oscillator

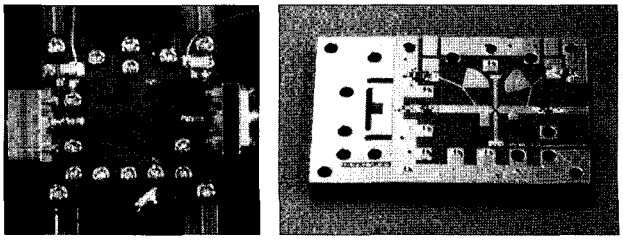

Fig. 12. Photo of designed PCR oscillator.

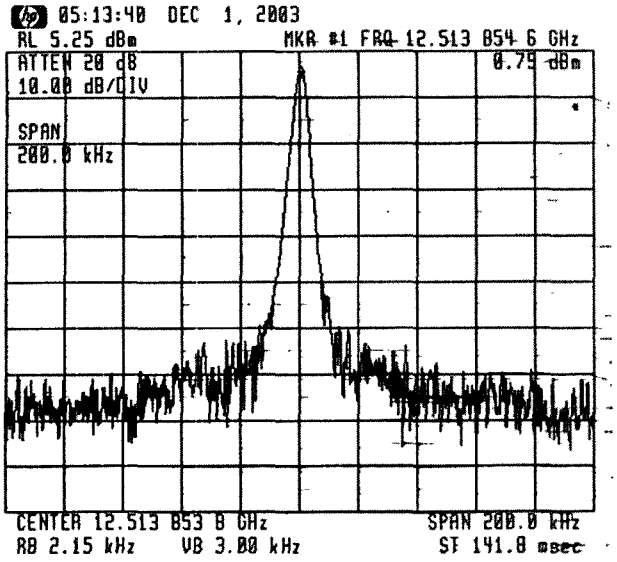


Fig. 13. Measured data of PCR oscillator at span 200 kHz.

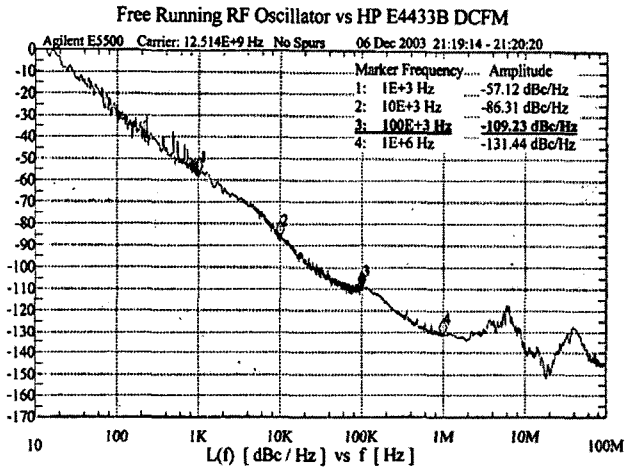


Fig. 14. Measured phase noise of PCR oscillator.

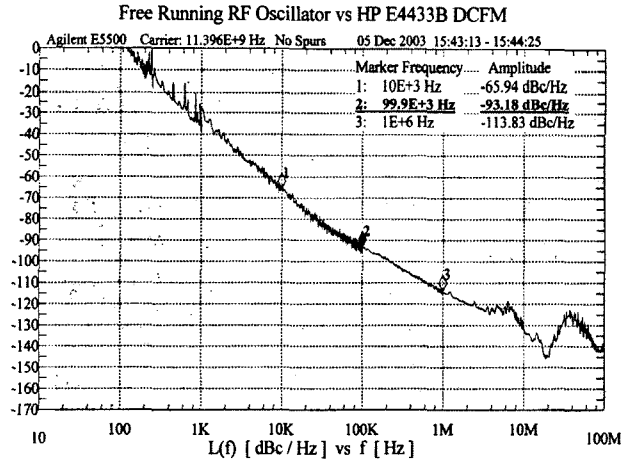


Fig. 15. Measured phase noise of MSR oscillator.

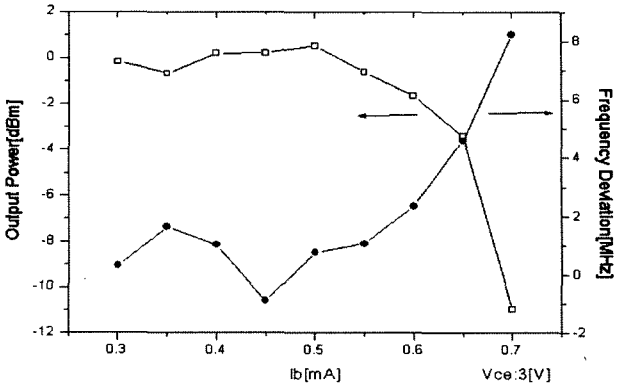


Fig. 16. Base bias dependence of PCR oscillator output-power and frequency deviation from 12.5 GHz.

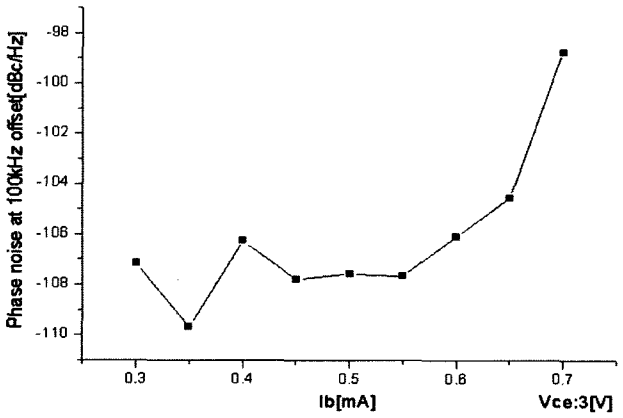


Fig. 17. Base bias dependence of PCR oscillator phase noise from 12.5 GHz.

Table 4. Measured the parameters of oscillator ($Ib$=497 $\mu$A, $Vce$=3 V).

| | | Measured data | |
|---|---|---|---|
| | | PCR | MSR |
| Frequency [GHz] | | 12.51 | 11.39 |
| Output Power [dBm] | | 2.767 | −1.472 |
| Second harmonic suppress [dBc] | | −35.02 | −25.5 |
| Phase noise [dBc/Hz] | 10 kHz | −86.31 | −65.95 |
| | 100 kHz | −109.23 | −93.18 |
| | 1 MHz | −131.44 | −113.83 |

with the PCR compared to the conventional microstrip resonator(MSR) in Fig. 15.

In Table 5, the PCR oscillator is compared with the published paper. In the SiGe device, the phase noise of the PCR oscillator shows the reduction of phase noise by 11 dBc/Hz @100 kHz offset compared to that of the

Table 5. The phase noise of published oscillator.

| | Frequency | Output-power | Phase noise (@100 kHz) |
|---|---|---|---|
| DR[9] | 12.7 GHz | −10 dBm | −124 dBc/Hz |
| Hair-pin[10] | 9 GHz | 5 dBm | −92 dBc/Hz |
| PCR | 12.514 GHz | 2.767 dBm | −109.23 dBc/Hz |

published hair-pin oscillator[10].

## VII. Conclusions

In this paper, a design method for oscillator using the planar cavity resonator is investigated, fabricated and tested to obtain the low phase noise oscillator utilizing hybrid integration on all planar printed circuit board.

The output power of the oscillator is 2.76 dBm and the phase noise is −109.23 dBc/Hz @100 kHz offset. Although this PCR oscillator shows higher phase noise than DR oscillator, the phase noise level of the PCR oscillator is lower than that of the MSR oscillator and the oscillator based on MEMS resonator[6].

That is, 1) The PCR oscillator makes an integration circuit better than the DR oscillator. 2) The fabrication processing of the PCR has easier than that of the MEMS resonator. 3) The $Q$ of PCR is higher than that of MSR. Therefore, PCR shows a noticeable reduction of phase noise and expects to the possibility of the easy fabrication and inexpensive mass production.

## References

[1] O. Llopis, G. Cibiel, Y. Kersale, M. Regis, M. Chaubet, and V. Giordano, "Ultra low phase noise sapphire-SiGe HBT oscillator", *IEEE Microwave and Wireless Components Letters*, vol. 12, no. 5, pp. 157-159, May 2002.

[2] B. V. Haaren, M. Regis, O. Llopis, and L. Escotte, "Low frequency noise properties of SiGe HBT's and application to ultra-low phase-noise oscillators", *IEEE Trans. on Microwave Theory and Tech.*, vol. 46, no. 5, pp. 647-652, May 1998.

[3] R. Jones, V. Estrick, "Low phase noise dielectric resonator oscillator", *Forty-Fourth Annual Symposium on Frequency Control IEEE 1990*, pp. 549-554.

[4] Y. W. Kwon, C. G. Cheon, N. T. Kim, C. W. Kim, I. S. Song, and C. M. Song, "A Ka-band MMIC oscillator stabilized with a micromachined cavity", *Microwave and Guided Wave Letters, IEEE [see also IEEE Microwave and Wireless Components Letters]*, vol. 9, no. 9, pp. 360-362, Sep. 1999.

[5] A. R. Brown, G. M. Rebeiz, "A Ka-band micromachined low-phase-noise oscillator", *Microwave Theory and Tech., IEEE Trans. on*, vol. 47, no. 8, pp. 1504-1508, Aug. 1999.

[6] J. Papapolymerou, J. C. Cheng, J. East, and L. P. B. Katehi, "A micromachined high-Q X-band resonator", *Microwave and Guided Wave Letters, IEEE [see also IEEE Microwave and Wireless Components Letters]*, vol. 7, no. 6, pp. 168-170, Jun. 1997.

[7] G. Cibiel, M. Regis, O. Llopis, Y. Kersale, V. Giordano, H. Lafontaine, R. Plana, and M. Chaubet, "Ultra low phase sige HBT application to a C band sapphire resonator oscillator", *2002 IEEE MTT-S Digest*, pp. 691-694.

[8] M. Regis, O. Llopis, and J. Graffeuil, "Nonlinear modeling and design of bipolar transistors ultra-low phase-noise dielectric-resonator oscillators", *IEEE Transactions on Microwave Theory and Tech.*, vol. 46, no. 10, pp. 1589-1593, Oct. 1998.

[9] M. Regis, "Design of low phase noise Ku-band oscillators using sige LPT16ED transistor", SiGe Semiconductor, Application note, Document#07AN 001 Rev., no. 1.

[10] L. Dussopt, G. M. Rebeiz, "A very low phase noise SiGe VCO at X-band frequencies", *Silicon Monolithic Integrated Circuits in RF Systems, 2001. Digest of Papers. 2001 Topical Meeting*, pp. 219-214, Sep. 2001.

[11] Y. T. Lee, J. S. Lim, C. S. Kim, D. Ahn, and S. W. Nam, "A compact-size microstrip spiral resonator and its application to microwave oscillator", *Microwave and Wireless Components Letters, IEEE [see also IEEE Microwave and Guided Wave Letters]*, vol. 12, no. 10, pp. 39-41, Oct. 2002.

[12] U. Guttich, A. Gruhle, "A Si-SiGe HBT dielectric resonator stabilized microstrip oscillator at X-band frequencies", *IEEE Microwave and Guided Wave Letters*, vol. 2, no. 7, pp. 281-283, Jul. 1992.

Jae-Won Lee

received the B.S. degree in electronic engineering from Hankuk Aviation University, Gyeonggi-do, Korea, in 2002 and the M.S. degree in the department of mechatronics from GIST(Gwangju Institute of Science Technology), Gwangju, Korea in 2004. Currently, he is a junior research engineer in Samsung Thales Co., LTD, Gyeonggi-do, Korea. His current interests include microwave/millimeter wave device and the design of system.

Yong-Hoon Kim

received the B.S. degree in radio science &engineering from Kyung Hee University, Seoul, Korea, in 1974, the M.S. degree in electronic engineering from Yon Sei University, Seoul, Korea, in 1976 and the Ph.D. degree from Stuttagrt University, Germany, in 1990. From 1990 to 1994, he was a senior research engineer in KARI(Korea Aerospace Research Institute). Currently, he is professor in the department of mechatronics at GIST(Gwangju Institute of Science Technology), Gwangju, Korea, and is representative in Millisys. Co., LTD, Gwangju, Korea. His research interests include microwave/millimeter wave device and system, applications of communication and communications satellite.